

---

---

# Long-Acting Somatostatin Analog Therapy Differentially Alters $^{68}\text{Ga}$ -DOTATATE Uptake in Normal Tissues Compared with Primary Tumors and Metastatic Lesions

Narjess Ayati<sup>1</sup>, Sze Ting Lee<sup>2</sup>, Rasoul Zakavi<sup>1</sup>, Kunthi Pathmaraj<sup>2</sup>, Louai Al-Qatawna<sup>3</sup>, Aurora Poon<sup>2</sup>, and Andrew M. Scott<sup>2,4,5</sup>

<sup>1</sup>Nuclear Medicine Research Centre, Mashhad University of Medical Sciences, Mashhad, Iran; <sup>2</sup>Department of Molecular Imaging and Therapy, Austin Health, Heidelberg, Victoria, Australia; <sup>3</sup>Nuclear Medicine and Cyclotron Unit, King Hussein Medical Center, Jordanian Royal Medical Services, Amman, Jordan; <sup>4</sup>Olivia Newton-John Cancer Research Institute, and School of Cancer Medicine, La Trobe University, Melbourne, Australia; and <sup>5</sup>Department of Medicine, University of Melbourne, Austin Health, Heidelberg, Victoria, Australia

Synthetic somatostatin analogs have been posed as a potential source of error in somatostatin receptor imaging through interference with tumor detection; however, experimental models and clinical studies have shown a complex mechanism of the effect of octreotide on tumors. The aim of this study was to assess whether  $^{68}\text{Ga}$ -DOTATATE uptake before treatment with long-acting somatostatin analogs differs from that after treatment. **Methods:** Thirty patients (15 men; age [mean  $\pm$  SD], 64.6  $\pm$  13.4 y) who had intermediately differentiated to well-differentiated neuroendocrine tumors and who underwent  $^{68}\text{Ga}$ -DOTATATE PET/CT scanning before and after receiving long-acting repeatable octreotide (Sandostatin LAR) were included in the study. The  $\text{SUV}_{\text{max}}$  and  $\text{SUV}_{\text{mean}}$  of healthy target organs, residual primary tumor, and up to 5 lesions with the highest  $\text{SUV}_{\text{max}}$  in each organ were compared before and after octreotide treatment. **Results:** The mean time interval between the 2  $^{68}\text{Ga}$ -DOTATATE studies was 9.6  $\pm$  7.2 mo, and the mean time gap between the last Sandostatin LAR injection and the second  $^{68}\text{Ga}$ -DOTATATE study was 25.1  $\pm$  14.8 d. The pretreatment mean  $\text{SUV}_{\text{max}}$  and  $\text{SUV}_{\text{mean}}$  were both significantly higher in the thyroid, liver, and spleen ( $P < 0.05$ ) than the values measured after the administration of Sandostatin LAR. No significant differences were found among the uptake indices for residual primary tumor or any metastatic lesions in the liver, bone, lung, or lymph nodes before and after Sandostatin LAR administration ( $P > 0.05$ ). **Conclusion:** Long-acting octreotide treatment diminished  $^{68}\text{Ga}$ -DOTATATE uptake in the liver, spleen, and thyroid but did not compromise tracer uptake in residual primary tumor and metastatic lesions. These findings have a direct impact on the interpretation of  $^{68}\text{Ga}$ -DOTATATE PET/CT scans.

**Key Words:** neuroendocrine tumor; somatostatin receptor imaging;  $^{68}\text{Ga}$ -DOTATATE; octreotide; somatostatin analogs

**J Nucl Med 2018; 59:223–227**

DOI: 10.2967/jnumed.117.192203

**P**ET/CT with  $^{68}\text{Ga}$ -DOTATATE plays a pivotal role in neuroendocrine tumor (NET) management (1), providing incremental data compared with  $^{111}\text{In}$ -pentetate (Octreoscan; Mallinckrodt) and conventional imaging (2) and better sensitivity and specificity than  $^{18}\text{F}$ -FDG PET imaging for neuroendocrine neoplasms (3,4). The clinical indications include primary tumor localization (5), metastatic disease detection, and response monitoring (6). In addition, somatostatin receptor (SSTR) imaging has established value in the prediction of response to treatment (7).

Synthetic somatostatin analogs have been shown to have clinical utility in patients with functionally active NETs by prolonging the time to progression (8,9) and controlling symptoms (10). However, somatostatin analogs may confound the interpretation of SSTR imaging data because they interfere with tumor detection (11) by saturating SSTRs in tumors (12). Experimental models and some human studies have shown the upregulation of SSTR expression in tumor cells and alterations in the internalization of subtype 2 SSTRs after the introduction of somatostatin analog treatment (12–15). These observations may result partly from the complex mechanism of the effect of octreotide on tumoral lesions, which may be different from the mechanism of the effect of the compound on normal target tissues (16). Clinical studies in this regard have been limited with respect to the number of patients evaluated and have mainly assessed the impact of octreotide treatment on Octreoscan imaging (17,18). Only 1 study has investigated the effect of octreotide on PET tracer SSTR imaging (19).

The aim of this study was to assess whether  $^{68}\text{Ga}$ -DOTATATE uptake in target organs, residual primary NETs, and metastases before treatment with long-acting somatostatin analogs differs from that after treatment.

## MATERIALS AND METHODS

All patients who had intermediately differentiated to well-differentiated NETs, who underwent  $^{68}\text{Ga}$ -DOTATATE PET/CT scans before and after receiving somatostatin analog treatment, and who were referred to Austin Hospital (Heidelberg, Victoria, Australia) for restaging from December 2013 to July 2016 were included in the study. Thirty patients (15 women and 15 men; age [mean  $\pm$  SD], 64.6  $\pm$  13.4 y; age range, 32–86 y) were studied. The study was approved by the Austin

---

Received Feb. 27, 2017; revision accepted Jun. 28, 2017.

For correspondence contact: Andrew M. Scott, Department of Molecular Imaging and Therapy, Austin Health, 145 Studley Rd., Heidelberg, Victoria 3084, Australia.

E-mail: andrew.scott@austin.org.au

Published online Jul. 20, 2017.

COPYRIGHT © 2018 by the Society of Nuclear Medicine and Molecular Imaging.

Health Human Research Ethics Committee, and all subjects signed a written informed consent form.

Demographic data were collected, and all disease-related information—including tumor type, grade, and primary site; any treatment received between the 2 scans; exact somatostatin analog dosing; the time interval from the last treatment to the second study; and the interval between the 2 studies—was recorded. If the patient had more than 1 scan before and more than 1 scan after octreotide administration, the last scan before and the first scan (not the final scan) after treatment were chosen for analysis. This selection minimized the time interval between 2 compared scans. All patients received long-acting repeatable octreotide (Sandostatin LAR; Novartis) at a dose of 30 mg every 4 wk, except for 1 patient, who received a 60-mg dose on the same time line.

$^{68}\text{Ga}$ -DOTATATE was synthesized using established techniques (7).  $^{68}\text{Ga}$  was eluted from a  $^{68}\text{Ge}/^{68}\text{Ga}$  generator (ITG), and high-performance liquid chromatography and radio-thin-layer chromatography were used to assess the purity and verify the identity of the final product. The radiochemical purity of the final product was greater than 90%.

Sixty minutes after the injection of 110–185 MBq of  $^{68}\text{Ga}$ -DOTATATE, whole-body scans were obtained from the skull vertex to the upper thighs on a Gemini Time-of-Flight PET/CT scanner (Philips). After the transmission scans, 3-dimensional PET acquisition was performed for 2–3 min per bed position. Low-dose CT was performed, and the data were used for attenuation correction and lesion localization. An iterative reconstruction algorithm was applied for image reconstruction.

Images were analyzed using a dedicated software package (version 6.4.5; MIM Software Inc.). The  $\text{SUV}_{\text{mean}}$  and  $\text{SUV}_{\text{max}}$  of healthy target organs, including the liver, spleen, adrenal glands, thyroid, and pituitary gland, were analyzed in both scans for each patient. If there was evidence of metastasis in an organ, then it was excluded from the analysis, except for the liver. In livers with up to 3 focal sites of metastasis, a region of interest was drawn distal to the lesions at the same location in both  $^{68}\text{Ga}$ -DOTATATE studies, and the indices were considered to represent the values of the healthy target organ.  $\text{SUV}_{\text{mean}}$  and  $\text{SUV}_{\text{max}}$  were also calculated in the primary site of the tumor (if remaining) and in up to 5 lesions that had the highest SUV in each organ and were present in both scans (Fig. 1). To prevent partial-volume effects, we excluded subcentimeter lesions from the analysis.

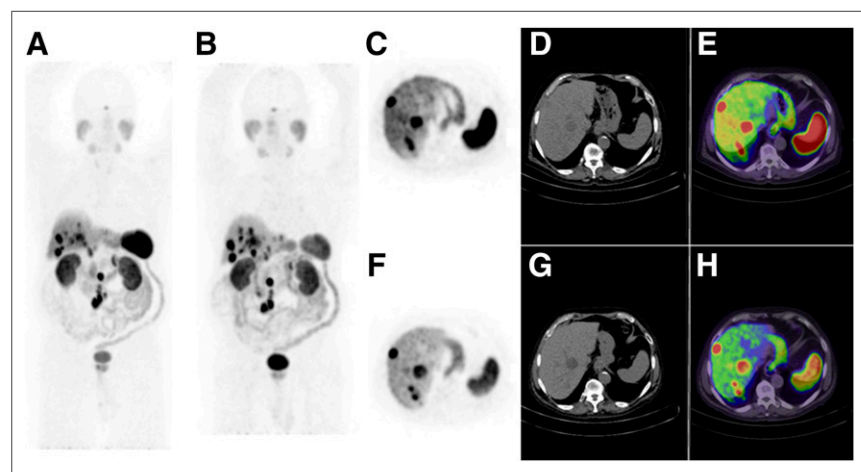


**FIGURE 1.**  $^{68}\text{Ga}$ -DOTATATE PET whole-body maximum-intensity projection images in patient with small-bowel carcinoid tumor before (A) and after (B) 12 mo of treatment with Sandostatin LAR (30 mg/4 wk). The post treatment scan showed reduced uptake of  $^{68}\text{Ga}$ -DOTATATE in normal liver, spleen, and thyroid, also seen in transaxial PET, CT, and fused images before (C–E) and after (F–H) treatment. Both primary and metastatic lesions showed similar uptake of  $^{68}\text{Ga}$ -DOTATATE, with the  $\text{SUV}_{\text{mean}}$  of the hottest lesion 30.6 in the first study and 31.8 in the second study.

SPSS software (version 16.0; SPSS Inc.) was used for data analysis. Descriptive statistics were used to describe the data. Quantitative variables were compared between 2 groups using paired-sample *t* tests, and qualitative variables were assessed using the McNemar test. A *P* value of less than 0.05 was considered significant in all comparisons.

## RESULTS

Primary tumor sites are shown in Table 1. Tumor grade and Ki-67 were formally reported in 18 and 14 patients, respectively (Table 1).

The mean time interval between the 2 studies was  $9.6 \pm 7.2$  mo (range, 3–32 mo), and the mean time gap between the last Sandostatin LAR injection and the second study was  $25.1 \pm 14.8$  d (range, 1–59 d). Our analysis of  $^{68}\text{Ga}$ -DOTATATE studies in individual patients revealed stable disease in 73.3% (22/30), disease progression in 20.0% (6/30), and a partial response in 6.7% (2/30).

The mean  $\text{SUV}_{\text{max}}$  and  $\text{SUV}_{\text{mean}}$  in normal organs were compared before and after Sandostatin LAR administration; the results are shown in Table 2. After Sandostatin LAR treatment, the mean  $\text{SUV}_{\text{max}}$  significantly decreased in the thyroid, liver, and spleen ( $P < 0.05$ ), whereas no significant differences were noted in the pituitary and adrenal glands (*P* was not significant). Figure 1 shows  $^{68}\text{Ga}$ -DOTATATE PET/CT images from a representative patient before and after Sandostatin LAR treatment.

No significant differences in the  $\text{SUV}_{\text{max}}$  were found in any metastatic lesions in the liver, bone, lung, or lymph nodes before and after Sandostatin LAR administration ( $P > 0.05$ ). We analyzed the  $\text{SUV}_{\text{mean}}$  of the metastatic lesions before and after Sandostatin LAR treatment. There were no significant differences in the  $\text{SUV}_{\text{mean}}$  before and after Sandostatin LAR treatment ( $P > 0.05$ ). Table 3 shows the mean pre- and posttreatment  $\text{SUV}_{\text{max}}$  and  $\text{SUV}_{\text{mean}}$  for the metastatic lesions examined. We compared the  $\text{SUV}_{\text{max}}$  and  $\text{SUV}_{\text{mean}}$  for the hottest lesion (i.e., with the highest  $\text{SUV}_{\text{max}}$ ) in each scan before and after Sandostatin LAR therapy. The mean  $\text{SUV}_{\text{max}}$  for the hottest lesion was  $26.8 \pm 14.7$  before Sandostatin LAR therapy and  $27.8 \pm 13.3$  after Sandostatin LAR therapy ( $P = 0.58$ ), and the mean  $\text{SUV}_{\text{mean}}$  was  $19.9 \pm 10.2$  and  $20.3 \pm 9.1$ , respectively ( $P = 0.79$ ). For the residual primary tumors, the mean  $\text{SUV}_{\text{max}}$  was  $15.3 \pm 8.0$  before Sandostatin LAR therapy and  $13.3 \pm 6.9$  after Sandostatin LAR therapy ( $P = 0.087$ ), and the mean  $\text{SUV}_{\text{mean}}$  was  $12.4 \pm 5.9$  and  $11.0 \pm 4.8$ , respectively ( $P = 0.179$ ).

## DISCUSSION

In the present study, the effect of long-acting somatostatin analog treatment on  $^{68}\text{Ga}$ -DOTATATE uptake in patients with NETs was assessed. To our knowledge, this study is the first to assess  $^{68}\text{Ga}$ -DOTATATE uptake in the same subset of patients before and after the administration of a long-acting somatostatin analog.

SSTR imaging guidelines recommend the withdrawal of octreotide therapy before imaging because of the possibility of interference of cold octreotide with tracer uptake in tumor cells, caused by competition for receptor occupancy as well as SSTR blockade (11,20). However, in vitro

**TABLE 1**  
**Characteristics of Primary Tumor, Metastatic Lesions, and Treatment**

Characteristic	Number of patients	Percentage of patients
<b>Primary site of tumor</b>		
Small bowel	19	63.3
Pancreas	3	10.0
Lung	2	6.7
Appendix	1	3.3
Colon	1	3.3
Unknown	4	13.3
<b>Primary tumor present</b>		
First scan	16	53.3
Second scan	10	33.3
<b>Tumor grading</b>		
Grade I	4	13.3
Grade II	12	40.0
Grade III	2	6.7
N/A	12	40.0
<b>Percentage of Ki-67</b>		
<5	3	10.0
5–10	6	20.0
10–20	2	6.7
20–30	3	10.0
N/A	16	53.3
<b>Treatment</b>		
No treatment	19	63.3
Tumor resection	10	33.3
Surgery + SiR-Spheres	1	3.3
<b>Interval treatment (other than Sandostatin LAR)</b>		
No treatment	21	70.0
Surgery	6	20.0
Chemotherapy	3	10.0
<b><sup>68</sup>Ga-DOTATATE PET/CT result</b>		
<b>&lt;3 focal lesions</b>		
First scan	5	16.7
Second scan	6	20.0
<b>≥3 focal lesions</b>		
First scan	25	83.3
Second scan	24	80.0
<b>Metastatic involvement*</b>		
<b>Liver</b>		
First scan	20	66.7
Second scan	21	70.0
<b>Lymph node</b>		
First scan	21	70.0
Second scan	23	76.7
<b>Lung</b>		
First scan	2	6.7
Second scan	2	6.7
<b>Bone</b>		
First scan	6	20.0
Second scan	7	23.3
<b>Adnexa</b>		
First scan	1	3.3
Second scan	1	3.3
<b>Pancreas</b>		
First scan	1	3.3
Second scan	1	3.3
<b>Analyzed lesions†</b>		
Total	160	
Liver	73	
Lymph node	60	
Bone	23	
Lung	2	
Other	2	

\*Frequency of tumoral involvement of each organ detected by <sup>68</sup>Ga-DOTATATE PET/CT.

†Number of tumoral lesions in 2 <sup>68</sup>Ga-DOTATATE PET/CT studies.

N/A = not available.

studies (14,21–23), in vivo animal studies (24), and human studies (25) have all shown that octreotide treatment strongly triggers agonist-induced internalization of subtype 2 SSRT and alters the degree of SSTR expression in NETs.

In the present study, we showed that primary tumor sites and metastatic lesions exhibited similar <sup>68</sup>Ga-DOTATATE uptake before and after the administration of a long-acting somatostatin analog; however, <sup>68</sup>Ga-DOTATATE uptake was significantly reduced in the liver, spleen, and thyroid after the treatment. Our findings suggest that pretreatment with somatostatin analogs does not affect the detection of metastatic disease and, in fact, reduces background uptake in normal organs; the later effect enhances the tumor-to-background ratio and facilitates tumor detection. Possible explanations for our findings are the difference in the internalization patterns in normal tissues and tumor cells (25) and the potential upregulation of SSTR expression after somatostatin analog therapy. These mechanisms may compensate for each other and, consequently, negate possible decreases in <sup>68</sup>Ga-DOTATATE accumulation in metastatic lesions. Previous studies showed that NETs may have heterogeneous SSTR expression (25) and may respond differently to somatostatin analog treatment. To address this potentially confounding issue, we compared <sup>68</sup>Ga-DOTATATE uptake in the same lesions in individual patients and used both SUV<sub>mean</sub> and SUV<sub>max</sub> in our analysis.

The finding that there were no differences in adrenal and pituitary gland uptake before and after Sandostatin LAR treatment is interesting and is in agreement with the results of a previous study (18). However, significant differences in uptake were found in other normal organs (liver, spleen, and thyroid). This finding may have been due to physiologic variability in SSTR expression among different organs, as previously reported (26,27).

Two previous studies (17,18) investigated the effect of somatostatin analog treatment on <sup>111</sup>In-octreotide uptake and reported increases in tumor-to-background ratios after octreotide administration. However, both studies evaluated small populations (5 and 8 patients), and the tumor-to-background ratios measured in the latter study were quite heterogeneous—ranging from –79% to +0.87%, with an average of 50% (17,18). In the only previously published study on the effect of cold somatostatin analog treatment on the uptake of <sup>68</sup>Ga-labeled somatostatin analogs, Haug et al. (19) compared <sup>68</sup>Ga-DOTATATE uptake in 2 groups of patients with NETs: 1 group received long-acting octreotide treatment, whereas the other did not. Lower tracer uptake was found in normal liver and spleen tissues in the treated patients, whereas no significant difference in radio-tracer uptake was found in the metastatic lesions in the 2 groups (19). Intraindividual assessments of 9 patients also showed that uptake was unaffected after octreotide treatment. The results of the present study agree with the results obtained in the previous studies for both normal organ uptake and residual primary tumor activity.

To reduce the interfering effect of somatostatin analog treatment on SSTR imaging, some guidelines have recommended scheduling the imaging just before the next dose (28-d intervals); however, a previous study showed a steady-state profile for long-acting octreotide (28) with a long maintenance period of greater than 0.01 ng/mL/mg by week 12 or 13. Further studies comparing <sup>68</sup>Ga-DOTATATE uptake in patients with less and more than 28-d intervals between the last octreotide injection and imaging may be needed. Although the present study evaluated the effect of initial somatostatin analog treatment on <sup>68</sup>Ga-DOTATATE uptake in NETs, in many patients <sup>68</sup>Ga-DOTATATE PET studies are performed throughout the course of their treatment and at different times from somatostatin analog administration. The results of

**TABLE 2**  
Comparison of SUV<sub>max</sub> and SUV<sub>mean</sub> in Normal Organs Before and After Sandostatin LAR Treatment

Organ	No. of assessed organs	Type of SUV	SUV before treatment (mean ± SD)	SUV after treatment (mean ± SD)	P
Pituitary gland	30	SUV <sub>max</sub>	6.3 ± 2.8	6.2 ± 2.9	0.690
		SUV <sub>mean</sub>	4.3 ± 1.7	4.3 ± 1.9	0.940
Thyroid gland	30	SUV <sub>max</sub>	3.9 ± 1.4	2.6 ± 1.4	<0.001
		SUV <sub>mean</sub>	2.9 ± 1.2	1.9 ± 0.9	<0.001
Liver	17	SUV <sub>max</sub>	9.8 ± 2.3	7.6 ± 2.5	0.012
		SUV <sub>mean</sub>	7.1 ± 2.4	5.3 ± 1.7	0.015
Spleen	30	SUV <sub>max</sub>	24.5 ± 8.3	18.8 ± 7.3	0.001
		SUV <sub>mean</sub>	20.4 ± 7.0	15.3 ± 5.9	0.001
Adrenal gland	30	SUV <sub>max</sub>	14.9 ± 6.0	14.6 ± 5.2	0.771
		SUV <sub>mean</sub>	10.4 ± 4.6	10.6 ± 4.0	0.749

**TABLE 3**  
Mean SUV<sub>max</sub> and SUV<sub>mean</sub> in Metastatic Lesions Before and After Sandostatin LAR Treatment

Metastatic foci	No. of assessed lesions	Type of SUV	SUV before treatment (mean ± SD)	SUV after treatment (mean ± SD)	P
Liver	73	SUV <sub>max</sub>	20.7 ± 7.6	23.3 ± 9.3	0.153
		SUV <sub>mean</sub>	16.5 ± 5.7	17.5 ± 6.2	0.473
Lymph node	60	SUV <sub>max</sub>	18.3 ± 11.1	19.7 ± 16.1	0.876
		SUV <sub>mean</sub>	13.8 ± 9.0	14.2 ± 7.6	0.755
Bone	23	SUV <sub>max</sub>	26.0 ± 13.1	26.9 ± 10.7	0.571
		SUV <sub>mean</sub>	20.8 ± 12.0	21.2 ± 10.5	0.798
Lung	2	SUV <sub>max</sub>	10.3 ± 2.25	12.3 ± 5.35	0.776
		SUV <sub>mean</sub>	7.5 ± 2.3	9.2 ± 3.8	0.759

the present study provide important information on the potential effect of the time after treatment on initial <sup>68</sup>Ga-DOTATATE scans, which may be relevant to repeat imaging in individual patients.

In the present study, all patients were imaged using <sup>68</sup>Ga-DOTA-Tyr<sup>3</sup>-octreotate (<sup>68</sup>Ga-DOTATATE). Although variable affinity for SSTR subtypes has been reported for somatostatin analogs with different labeling, the imaging characteristics of these radiotracers are similar (29,30). Therefore, our results might be extended to all PET tracer–radiolabeled somatostatin molecules. The slow-growth nature of NETs as well as the potential antiproliferative properties of somatostatin analogs could imply differences in disease status. However, the present study was not designed to assess the therapeutic activity of somatostatin analogs or the ability of <sup>68</sup>Ga-DOTATATE to assess or predict a response.

Although the present study has the advantage of a comparison of data within the same subset of patients, because of the retrospective nature, the time interval between the 2 PET/CT imaging studies was quite long (9.6 mo). A prospective study with a shorter imaging interval (e.g., SSTR PET before somatostatin analog treatment and after the first or second administration) would be helpful.

## CONCLUSION

Long-acting somatostatin analog treatment decreased <sup>68</sup>Ga-DOTATATE uptake in the liver, spleen, and thyroid but did not

compromise <sup>68</sup>Ga-DOTATATE uptake in residual primary tumor or metastatic lesions. These findings support the sensitivity of SSTR imaging for the detection of metastasis in patients receiving somatostatin analog treatment.

## DISCLOSURE

No potential conflict of interest relevant to this article was reported.

## REFERENCES

- Virgolini I, Gabriel M, Kroiss A, et al. Current knowledge on the sensitivity of the <sup>68</sup>Ga-somatostatin receptor positron emission tomography and the SUV<sub>max</sub> reference range for management of pancreatic neuroendocrine tumours. *Eur J Nucl Med Mol Imaging*. 2016;43:2072–2083.
- Deppen SA, Liu E, Blume JD, et al. Safety and efficacy of <sup>68</sup>Ga-DOTATATE PET/CT for diagnosis, staging, and treatment management of neuroendocrine tumors. *J Nucl Med*. 2016;57:708–714.
- Mojtahedi A, Thamake S, Tworowska I, Ranganathan D, Delpassand ES. The value of <sup>68</sup>Ga-DOTATATE PET/CT in diagnosis and management of neuroendocrine tumors compared to current FDA approved imaging modalities: a review of literature. *Am J Nucl Med Mol Imaging*. 2014;4:426–434.
- Janssen I, Chen CC, Millo CM, et al. PET/CT comparing <sup>68</sup>Ga-DOTATATE and other radiopharmaceuticals and in comparison with CT/MRI for the localization of sporadic metastatic pheochromocytoma and paraganglioma. *Eur J Nucl Med Mol Imaging*. 2016;43:1784–1791.

5. Pruthi A, Pankaj P, Verma R, Jain A, Belho ES, Mahajan H. Ga-68 DOTANOC PET/CT imaging in detection of primary site in patients with metastatic neuroendocrine tumours of unknown origin and its impact on clinical decision making: experience from a tertiary care centre in India. *J Gastrointest Oncol.* 2016;7:449–461.
6. Velikyan I, Sundin A, Sorensen J, et al. Quantitative and qualitative intrapatient comparison of <sup>68</sup>Ga-DOTATOC and <sup>68</sup>Ga-DOTATATE: net uptake rate for accurate quantification. *J Nucl Med.* 2014;55:204–210.
7. Virgolini I, Ambrosini V, Bomanji JB, et al. Procedure guidelines for PET/CT tumour imaging with <sup>68</sup>Ga-DOTA-conjugated peptides: <sup>68</sup>Ga-DOTA-TOC, <sup>68</sup>Ga-DOTA-NOC, <sup>68</sup>Ga-DOTA-TATE. *Eur J Nucl Med Mol Imaging.* 2010;37:2004–2010.
8. Rinke A, Muller HH, Schade-Brittinger C, et al. Placebo-controlled, double-blind, prospective, randomized study on the effect of octreotide LAR in the control of tumor growth in patients with metastatic neuroendocrine midgut tumors: a report from the PROMID Study Group. *J Clin Oncol.* 2009;27:4656–4663.
9. Caplin ME, Pavel M, Cwikla JB, et al. Lanreotide in metastatic enteropancreatic neuroendocrine tumors. *N Engl J Med.* 2014;371:224–233.
10. Lancranjan I, Atkinson AB. Results of a European multicentre study with Sandostatin LAR in acromegalic patients. Sandostatin LAR Group. *Pituitary.* 1999;1:105–114.
11. Kwekkeboom DJ, Krenning EP, Scheidhauer K, et al. ENETS consensus guidelines for the standards of care in neuroendocrine tumors: somatostatin receptor imaging with <sup>111</sup>In-pentetreotide. *Neuroendocrinology.* 2009;90:184–189.
12. Ben-Shlomo A, Schmid H, Wawrowsky K, et al. Differential ligand-mediated pituitary somatostatin receptor subtype signaling: implications for corticotroph tumor therapy. *J Clin Endocrinol Metab.* 2009;94:4342–4350.
13. Arnold R, Trautmann ME, Creutzfeldt W, et al. Somatostatin analogue octreotide and inhibition of tumour growth in metastatic endocrine gastroenteropancreatic tumours. *Gut.* 1996;38:430–438.
14. Cescato R, Schulz S, Waser B, et al. Internalization of sst2, sst3, and sst5 receptors: effects of somatostatin agonists and antagonists. *J Nucl Med.* 2006;47:502–511.
15. Lesche S, Lehmann D, Nagel F, Schmid HA, Schulz S. Differential effects of octreotide and pasireotide on somatostatin receptor internalization and trafficking in vitro. *J Clin Endocrinol Metab.* 2009;94:654–661.
16. Bakker WH, Krenning EP, Reubi JC, et al. In vivo application of [<sup>111</sup>In-DTPA-D-Phe1]-octreotide for detection of somatostatin receptor-positive tumors in rats. *Life Sci.* 1991;49:1593–1601.
17. Dörr U, Rath U, Sautter-Bühl ML, et al. Improved visualization of carcinoid liver metastases by indium-111 pentetreotide scintigraphy following treatment with cold somatostatin analogue. *Eur J Nucl Med.* 1993;20:431–433.
18. Janson ET, Kalkner KM, Eriksson B, Westlin JE, Oberg K. Somatostatin receptor scintigraphy during treatment with lanreotide in patients with neuroendocrine tumors. *Nucl Med Biol.* 1999;26:877–882.
19. Haug AR, Rominger A, Mustafa M, et al. Treatment with octreotide does not reduce tumor uptake of <sup>68</sup>Ga-DOTATATE as measured by PET/CT in patients with neuroendocrine tumors. *J Nucl Med.* 2011;52:1679–1683.
20. Balon HR, Goldsmith SJ, Siegel BA, et al. Procedure guideline for somatostatin receptor scintigraphy with <sup>111</sup>In-pentetreotide. *J Nucl Med.* 2001;42:1134–1138.
21. Liu Q, Cescato R, Dewi DA, Rivier J, Reubi JC, Schonbrunn A. Receptor signaling and endocytosis are differentially regulated by somatostatin analogs. *Mol Pharmacol.* 2005;68:90–101.
22. Ginj M, Chen J, Walter MA, Eltschinger V, Reubi JC, Maecke HR. Preclinical evaluation of new and highly potent analogues of octreotide for predictive imaging and targeted radiotherapy. *Clin Cancer Res.* 2005;11:1136–1145.
23. Nock BA, Nikolopoulou A, Galanis A, et al. Potent bombesin-like peptides for GRP-receptor targeting of tumors with <sup>99m</sup>Tc: a preclinical study. *J Med Chem.* 2005;48:100–110.
24. Waser B, Tamma ML, Cescato R, Maecke HR, Reubi JC. Highly efficient in vivo agonist-induced internalization of sst2 receptors in somatostatin target tissues. *J Nucl Med.* 2009;50:936–941.
25. Reubi JC, Waser B, Cescato R, Gloor B, Stettler C, Christ E. Internalized somatostatin receptor subtype 2 in neuroendocrine tumors of octreotide-treated patients. *J Clin Endocrinol Metab.* 2010;95:2343–2350.
26. Kuyumcu S, Ozkan ZG, Sanli Y, et al. Physiological and tumoral uptake of <sup>68</sup>Ga-DOTATATE: standardized uptake values and challenges in interpretation. *Ann Nucl Med.* 2013;27:538–545.
27. Shastri M, Kayani I, Wild D, et al. Distribution pattern of <sup>68</sup>Ga-DOTATATE in disease-free patients. *Nucl Med Commun.* 2010;31:1025–1032.
28. Astruc B, Marbach P, Bouterfa H, et al. Long-acting octreotide and prolonged-release lanreotide formulations have different pharmacokinetic profiles. *J Clin Pharmacol.* 2005;45:836–844.
29. Johnbeck CB, Knigge U, Kjaer A. PET tracers for somatostatin receptor imaging of neuroendocrine tumors: current status and review of the literature. *Future Oncol.* 2014;10:2259–2277.
30. Poeppel TD, Binse I, Petersenn S, et al. Differential uptake of <sup>68</sup>Ga-DOTATOC and <sup>68</sup>Ga-DOTATATE in PET/CT of gastroenteropancreatic neuroendocrine tumors. *Recent Results Cancer Res.* 2013;194:353–371.